Progress In Electromagnetics Research M, Vol. 121, 49–62, 2023

A Low Profile Circularly Polarized Microstrip Antenna with Equilateral Triangular Patch and Parasitic Elements for Dual Application Band

Murari Shaw*

Abstract—In this research work, a low-profile microstrip patch antenna has been designed with broad circularly polarized resonant bandwidth. The designed antenna consists of an equilateral triangular-shaped radiating patch with two triangular coplanar parasitic elements along with a square-shaped ground plane. The unique feature of this antenna design is a generation of circularly polarized radiation by only optimum corner truncation of the two parasitic elements along with a small portion of the driver patch. The designed antenna can be used for (5.725–5.850 GHz) WLAN and (5.85–5.925 GHz) dedicated short-range communication applications with circularly polarized radiation property. The overall resonant bandwidth for ($S_{11} \leq -10$ dB) is 1.52 GHz 24.75% with a frequency range (5.38–6.90 GHz), and the circularly polarized resonant bandwidth for (Axial ratio ≤ 3 dB) is 240 MHz 4.13% with a frequency range (5.69–5.93 GHz). The gain of the antenna is 4 dB at 5.81 GHz and almost remains the same for the entire resonant bandwidth. The complete design of the antenna has been done using theoretical calculation and HFSS ver13 simulation software. After that, it has been fabricated, and different parameters have been measured using Vector Network Analyser. It has been found that the measured results are very much similar to the simulated results.

1. INTRODUCTION

Communication technology grows day by day at a fast pace due to which all the circuits, devices, and types of equipment used in it also changes and becomes more and more complex and diminishing. Since communication devices and equipment become smaller in size, the space allocated for the antenna in these devices and equipment is also shrinking. Hence, in order to adjust the antenna in these smaller spaces, the design of a smaller and more efficient antenna [1, 2] is required that can fit and be compatible with these advanced devices and circuits. With the advancement of communication technology, there is also a high demand for cheaper communication costs with lesser complexity. For this, low-priced equipment, devices, and circuits are needed in communication technology including antennas.

With the advancement of communication technology, there is also a very high demand for a single antenna that can cover more than one application band.

The position and orientation of the antenna used in wireless communication changes with the movement of the object on which it has been mounted on vehicles, airplanes, satellites, submarines, etc., due to which the polarization of the antenna also changes. This polarization change of the antenna causes polarization mismatch loss and also a multipath distortion. Therefore, circularly polarized antennas are needed in these mobile wireless communications which reduce polarization mismatch losses, multi-path distortion, and also transmitter & receiver orientation constraints [3–6].

Therefore, for today's modern wireless communication systems [7, 8], a low-profile, low-priced, circularly polarized antenna that can cover more than one application band is needed. As per the

Received 9 August 2023, Accepted 16 October 2023, Scheduled 14 November 2023

* Corresponding author: Murari Shaw (zmz_shaw@yahoo.co.in).
The author is with the Department of Electronics & Communication Engineering, Institute of Engineering & Management-Salt Lake, Kolkata 700091, West Bengal, India.

demand of today's advanced wireless communication systems, the microstrip patch antenna is very much suitable and attracs more and more research attention. After the literature survey, it has been found that a lot of research papers have been published with different designs and applications of microstrip patch antennas. The published designs of microstrip patch antennas have some merits and also some demerits. For example, in [9] and [10], slot antennas with coplanar waveguide (CPW)-feed have been designed for dual-band operations having high qualities, but the gain of the antennas is low due to bidirectional radiation. In [11] and [12], microstrip patch antennas with dual-band operations have been designed using metamaterial technology, but the demerit of the antennas is low peak gains. Two equilateral triangular microstrip antennas have been designed in [13] and [14]. By perturbation, one of the sides of the radiating patch using a narrow slit the designed antenna in [13] generated a circularly polarized (CP) bandwidth of 25 MHz (1.03%), and also by the truncated tip of a triangular radiating patch in [14] a circularly polarized bandwidth is generated. The generated CP bandwidth varies with the variation of the radiating patch size and also truncated tip size. The CP bandwidth generated by both the antennas is very narrow along with comparatively large size. Similarly, another equilateral triangular microstrip antenna has been designed in [15] that generated a circularly polarized bandwidth after the introduction of three triangular optimum-sized slots on the ground plane. The designed antenna has higher gain than the same dimension antenna with a truncated tip, but the CP bandwidth generated by it is narrow along with comparatively large size. In [16] and [17], a square radiating patch has been used to design a circularly polarized antenna, but the area required by the triangular patch antenna is less than the circular or square patch antenna for the same radiation properties at a certain frequency. In [18], a circularly polarized equilateral triangular patch antenna has been designed by attaching a tuning stub at the top vertex or at the center of the bottom of the triangular patch along with a cross-slot of equal lengths at the center of the patch to obtain a size reduction up to about 22%. The size of the antenna is still large along with the complexity of the design.

The above examples show that a large number of microstrip patch antennas have been designed and published in the literature, but there is still huge potential for further research and development. Therefore, more and more modified and well-designed antennas that could be more compatible with today's modern wireless communication systems can be developed and designed, which motivates the present work.

To fulfill and satisfy the requirement of advanced communication technology for low profile, low cost, circularly polarized bandwidth, and usable for more than one application band antenna, an equilateral triangular microstrip patch antenna is designed and proposed here. The proposed antenna generates a resonant frequency band with optimum radiation pattern and gain which is very much suitable and compatible with devices working on WLAN and dedicated short-range communication applications.

The design process of the antenna involves mainly four steps namely; theoretical study, design of the antenna using simulation software HFSS, optimization using simulated results, and experimental measurement of the fabricated antenna. All the above-mentioned steps are thoroughly described in the subsequent paragraphs.

2. ANTENNA DESIGN

The projected antenna as shown in Figs. 1(a), (b), and (c) consists of an equilateral triangular-shaped main radiating patch of 14.6 mm sides along with two triangular coplanar parasitic elements of (13.1, 11.3, and 6.6) mm sides. The distance of the parasites from the two sides of the main radiating patch is 0.7 mm. The distance of the final patch is 8.8 mm from the top, 8.5 mm from the bottom, and 7.7 mm from the left and right edges of the square substrate. Two opposite corners of the parasites have been cut out, and after truncation, the side length of the corners becomes 6.8 mm and 6.7 mm. The overall size of the proposed antenna is $30 \times 30 \times 3.2\,\text{mm}^3$ in which a thin copper sheet has been used to make a radiating patch and square-shaped ground plane. The square-shaped substrate between the patch and ground has been made using FR4 glass epoxy material whose relative permittivity (ε_r) is 4.4 and loss tangent ($\tan\delta$) 0.02. A 50 Ω co-axial probe SMA connector with a 0.63 mm inner radius and 1.45 mm outer radius has been attached to the antenna at a distance of 10.5 mm from the bottom edge, in order to energize it.

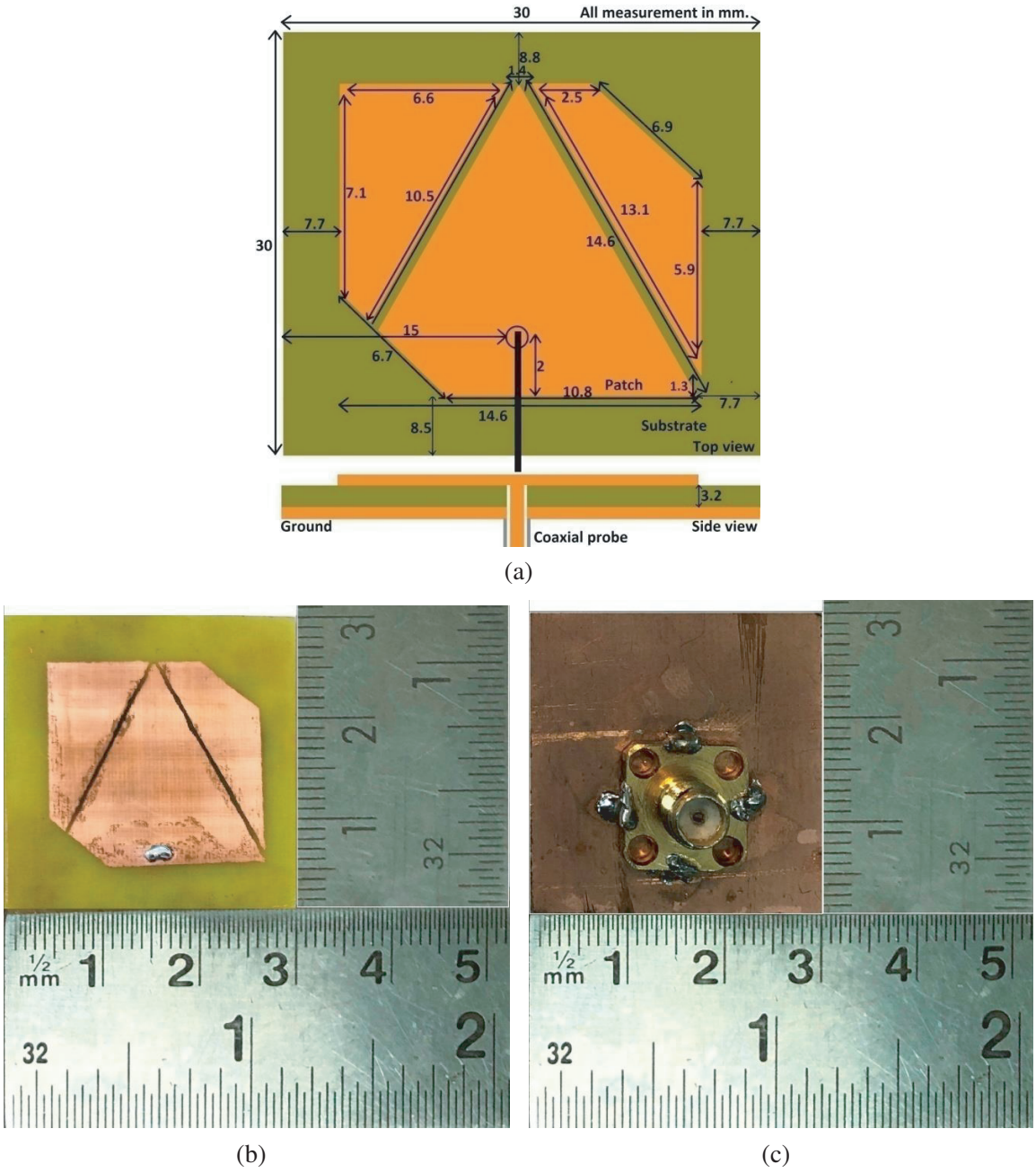

Figure 1. (a) Design of the proposed antenna. (b) Top view and (c) bottom view of the fabricated antenna.

3. ANTENNA DESIGN PROCEDURE WITH PARAMETRIC STUDY

For the design of the projected antenna, first, an equilateral triangle-shaped radiating patch has been selected, so that a low-profile antenna can be designed. It is known that the triangular patch antenna generates radiation characteristics similar to a rectangular patch antenna with a smaller size [19–21]. Therefore, the size of the designed antenna is smaller as per the requirement. After the selection of an equilateral triangle-shaped radiating patch, a theoretical calculation has been done with various side lengths of the radiating patch and mathematical Equations (1) and (2) [22, 23] to find the resonant

frequency of the antenna around WLAN (5.725–5.850 GHz) application band.

$$f_{mnl} = \frac{2C}{3a_{eff}\sqrt{\varepsilon_r}}\sqrt{(m^2+mn+n^2)} \quad (1)$$

$$a_{eff} = a\left[1+\frac{2h}{\pi a\varepsilon_r}\left\{\mathrm{In}\left(\frac{a}{2h}\right)+(1.41\varepsilon_r+1.77)+\frac{h}{a}(0.268\varepsilon_r+1.65)\right\}\right]^{\frac{1}{2}} \quad (2)$$

where

f_{mnl} = Resonant frequency,
m, n, l = Numbers represent modes of resonant frequency,
$C = 3\times10^{10}$ cm/sec,
a = Side length of the equilateral triangular patch,
a_{eff} = Effective side length,
h = Height of the substrate.

After various theoretical calculations, the side length of 14.6 mm of the radiating patch provided a primary resonant frequency (dominant mode TM_{10}) 5.72 GHz close to the needed result. Having a theoretical resonant frequency 5.72 GHz for a 14.6 mm side length, an equilateral triangular microstrip patch has been designed using simulator software HFSS with the same side length as mentioned above. After that, at the arbitrary probe position, the designed antenna is simulated and analyzed. After analysis, unwanted results have been found because of a mismatch of probe impedance and antenna impedance due to inappropriate probe position. Therefore, before making any modification in the conventional structure of the antenna, the probe position has been optimized by shifting the position of the probe 1 mm on the median of the equilateral triangular patch from base to top vertex and subsequent analysis of the results. Following the analysis of the results, it has been found that the impedance of the antenna and probe impedance is well matched at the probe position 2 mm above from the base on the median of the triangle. In this way, the optimum probe position has been found, and at that probe position, the simulated resonant frequency is 5.7 GHz almost the same as the theoretical resonant frequency with a resonant frequency range (5.5–5.91 GHz). The initial design of the antenna with reflection coefficient (S_{11}) and input impedance (Z_{11}) graph is displayed in Figs. 2(a), (b), and (c).

The above initial design of the projected antenna does not fulfill the requirement of the advanced communication devices. Therefore, it has been modified as per the requirement by using the techniques and process mentioned below.

3.1. Effect of Parasitic Elements

As the resonant bandwidth of the conventional antenna is narrow, it needs to be improved so that it can be used for more than one application band. For this purpose, two triangular parasitic elements have been added beside the two sides of the main radiating patch. The addition of the parasites enhanced the overall bandwidth of the antenna, because there has been coupling occurs between the fringing electromagnetic fields associated with radiating patch and parasites which ultimately causes wider bandwidth [24, 25]. The size and position of the added parasitic elements have been optimized by changing the sizes along with the positions and subsequent observation of the simulated results. Figs. 3(a), (b), (c), and (d) show the antenna with two optimized (both size and position) coplanar parasitic elements, simulated S_{11}, Z_{11}, and axial ratio graph.

After the addition of the parasites, the central resonant frequency shifts from 5.7 GHz to 5.45 GHz, and the resonant bandwidth is changed from 400 MHz to 480 MHz which can be observed in Fig. 4. Therefore, an overall bandwidth is increased by 80 MHz.

Hence, with the addition of the parasites the resonant bandwidth is improved, but the polarization of the antenna is linear which is evident from the high value of the axial ratio shown in Fig. 3(d). Therefore, in order to change the polarization from linear to circular, further modification has been done in the antenna structure.

3.2. Effect of Cutting the Opposite Corners

A microstrip patch antenna generates circular polarization radiation when its two orthogonal generated modes have the same amplitude, but the phase difference between them is ±90 degrees. From the

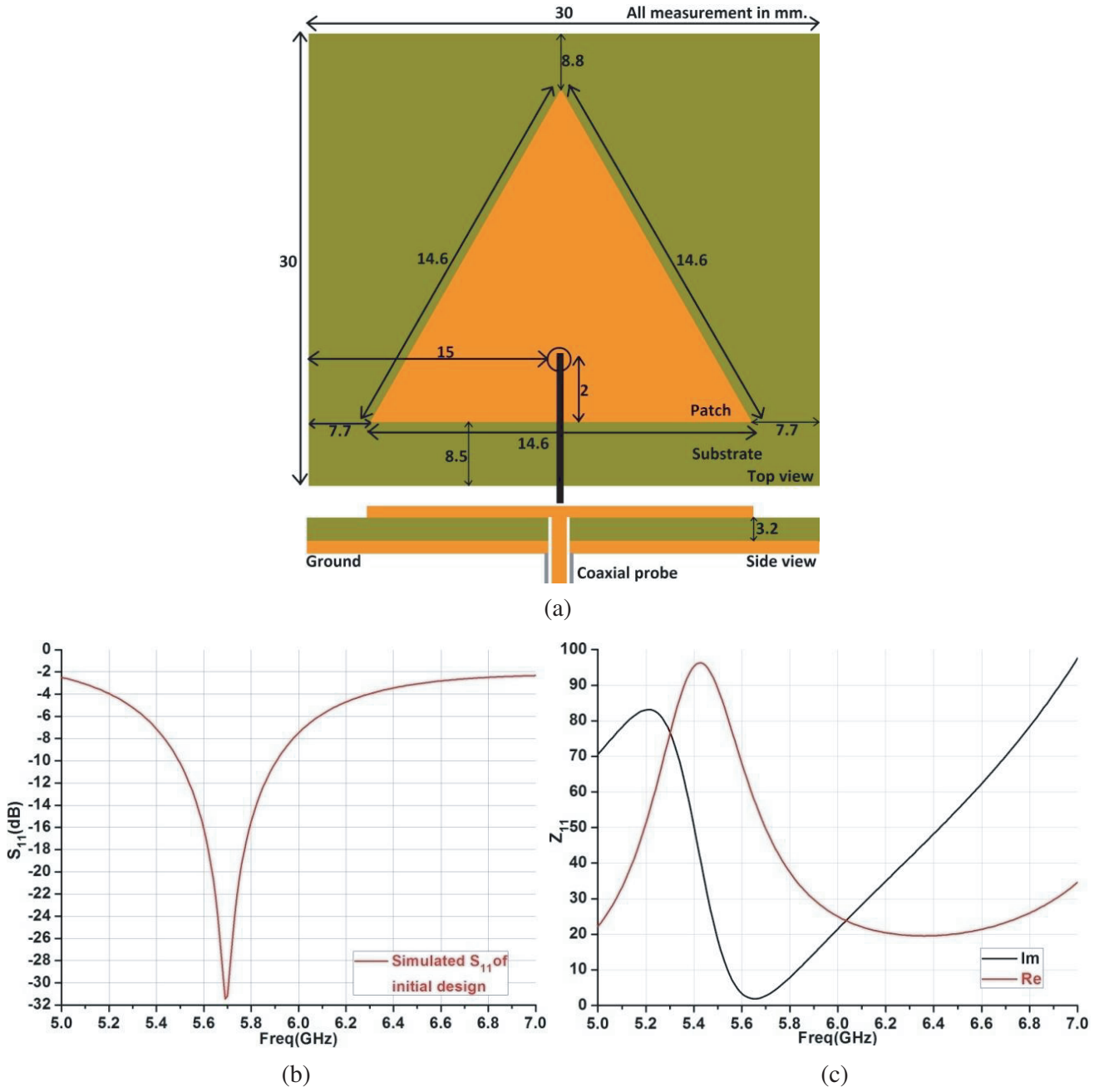

Figure 2. (a) Initial design of the proposed antenna with optimum probe position 2 mm above from base over the median. (b) S_{11} and (c) Z_{11} of the antenna at the above-mentioned probe position.

literature, it has been found that the truncation of the opposite corners of the square radiating patch generates orthogonal modes with equal amplitudes and 90° phase difference that facilitate the generation of the circular polarization radiation [26–28]. In the proposed antenna, after the addition of the coplanar parasites with a driver patch, the shape of the overall patch becomes closely similar to the square patch. Therefore, in order to change the polarization, the opposite corners of the parasitic elements along with a small portion of the driver patch has been truncated. Due to truncation, the effective surface current path of the revised patch in one direction is slightly shorter than that in the other direction. This causes the resonant frequency of a resonant mode in one direction slightly larger than that of the

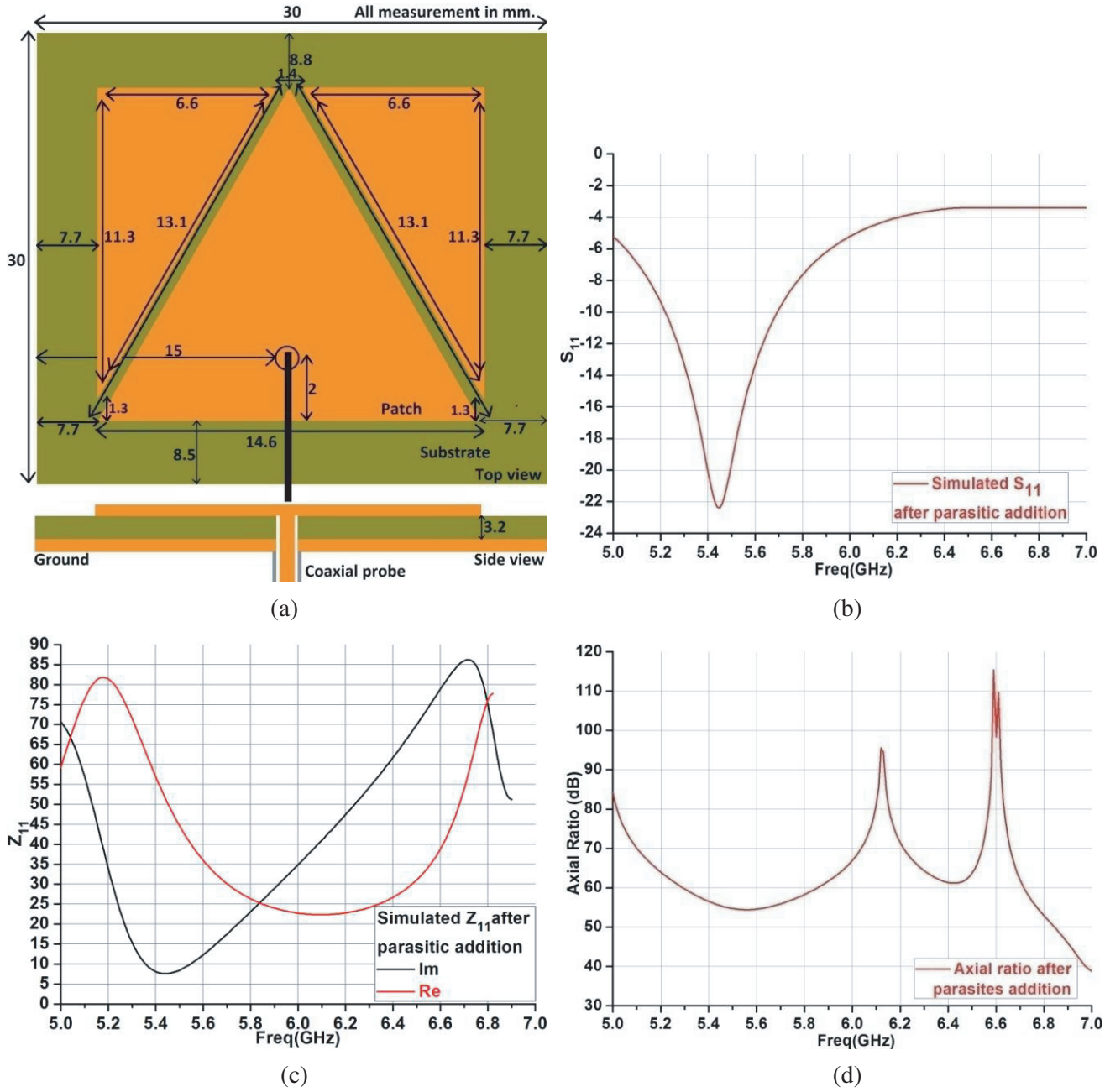

Figure 3. (a) Design of initial antenna with two optimized coplanar parasitic elements. (b) S_{11}, (c) Z_{11}, and (d) axial ratio of the antenna.

resonant frequency of the other direction resonant mode. Hence, the fundamental TM_{10} mode is split into two orthogonal near-degenerate modes with equal amplitude and 90° out of phase. In this way, corner truncation of the radiating patch makes the radiation polarization of the antenna circular. The corner truncation has been optimized by varying the cutting position of the corners and observing the corresponding simulated results. In this manner, the position and size of the corner truncation [29] have been optimized. Further modification in the dimension of the truncated corner shows unwanted results. The final design of the antenna with optimized corners is shown in Fig. 1. Its different parameters such as S_{11}, Z_{11}, axial ratio, phase difference, and surface current distribution of frequency 5.81 GHz at

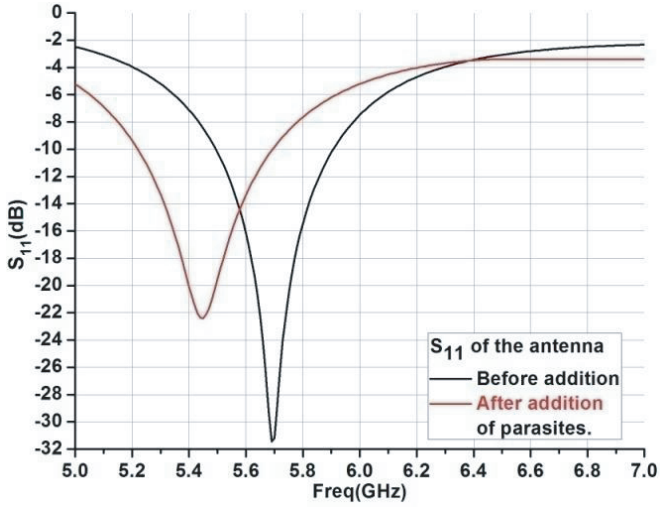

Figure 4. S_{11} of the antenna with the addition and without the addition of the parasites.

different time instants are shown in Figs. 5(a), (b), (c), (d), (e), (f), (g), and (h). It can be observed from the surface current distribution that after corner truncation the current distribution is altered in such a way that the antenna radiates a circularly polarized wave.

Axial ratio and phase difference graphs are used to show the clarity of the frequency range of the circular polarization. If the axial ratio is less than or equal to 3 dB and the phase difference around 90° over any frequency range, then the antenna is considered to have circular polarization in that frequency range. The axial ratio and phase difference graph are displayed in Figs. 5(c) and (d), and also axial ratio graphs in four different planes are shown in Figs. 6(a), (b), (c), and (d).

From both Figs. 5 and 6, it can be observed that the antenna has circular polarization in the (5.69–5.93 GHz) frequency bandwidth.

Following the above process, the final design of the antenna has been made, and a prototype of it has been fabricated as displayed in Figs. 1(b) & (c). The different parameters of the fabricated antenna have been measured using a Vector Network Analyzer benchtop (Model No.E5071B) and an anechoic chamber.

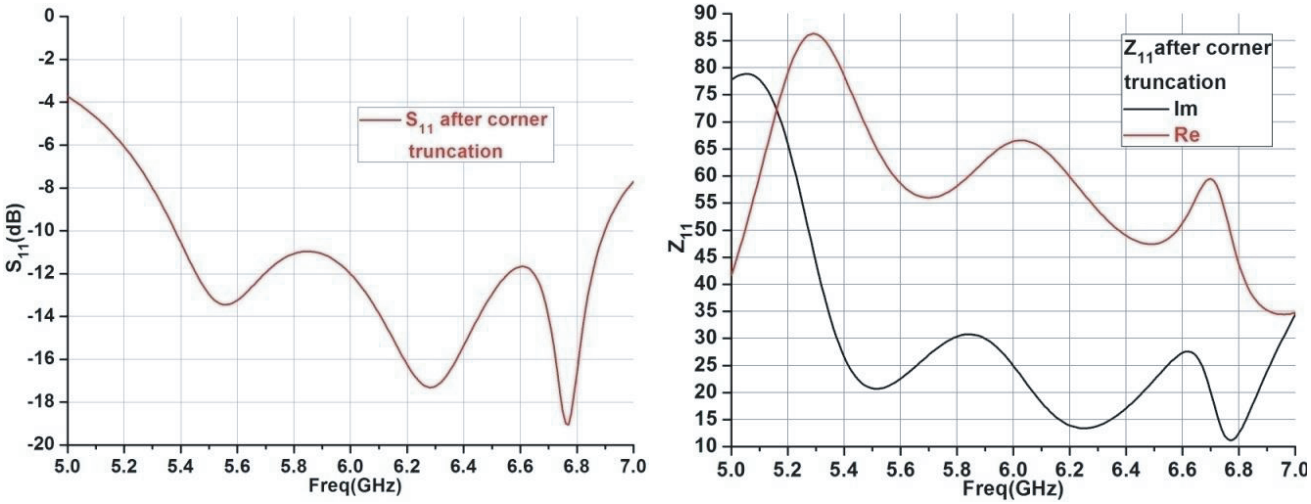

(a) (b)

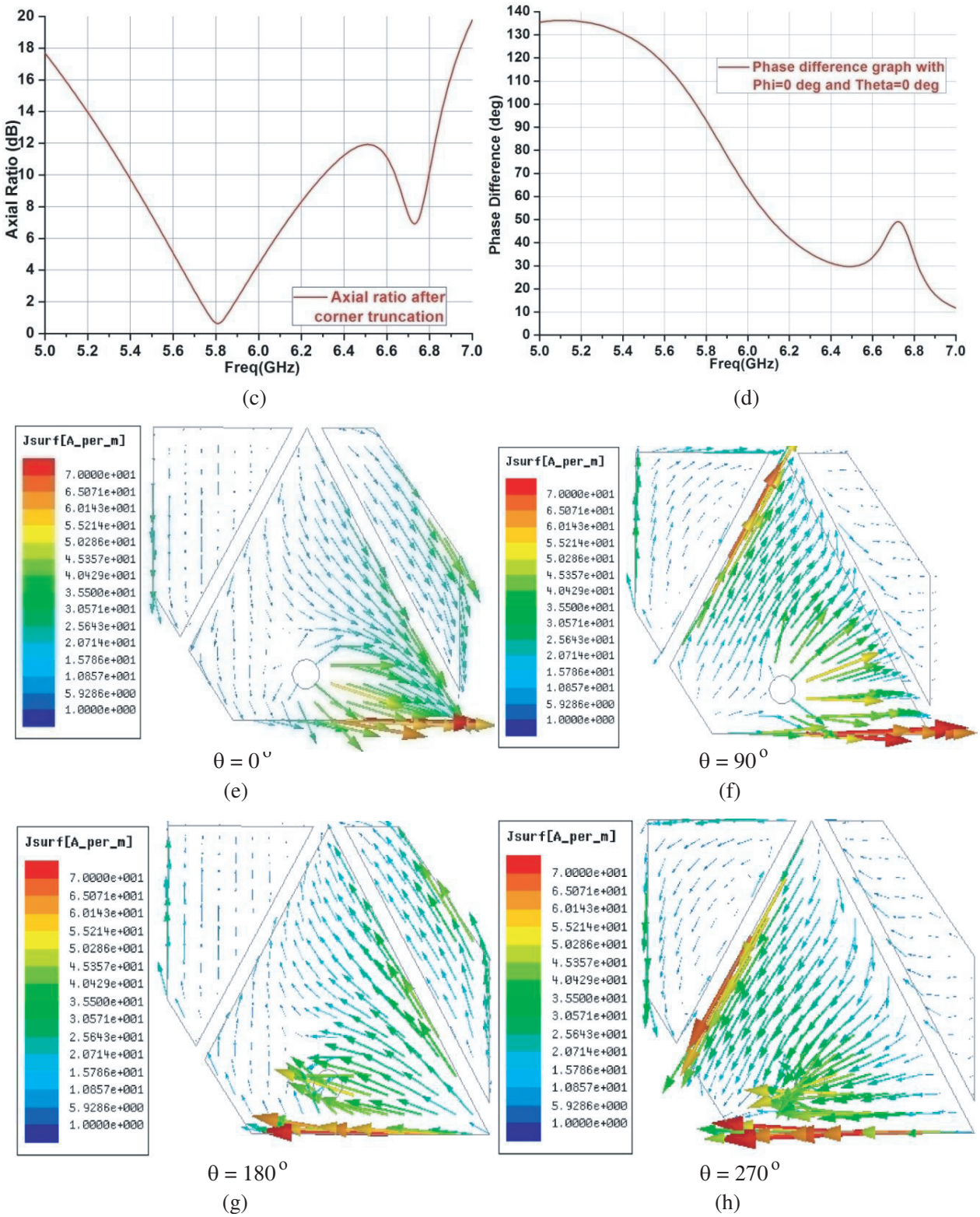

Figure 5. (a) S_{11}, (b) Z_{11}, (c) axial ratio, and (d) phase difference graph of the antenna after optimized corner truncation. (e), (f), (g), and (h) Simulated surface current distribution at 5.81 GHz for different time instants.

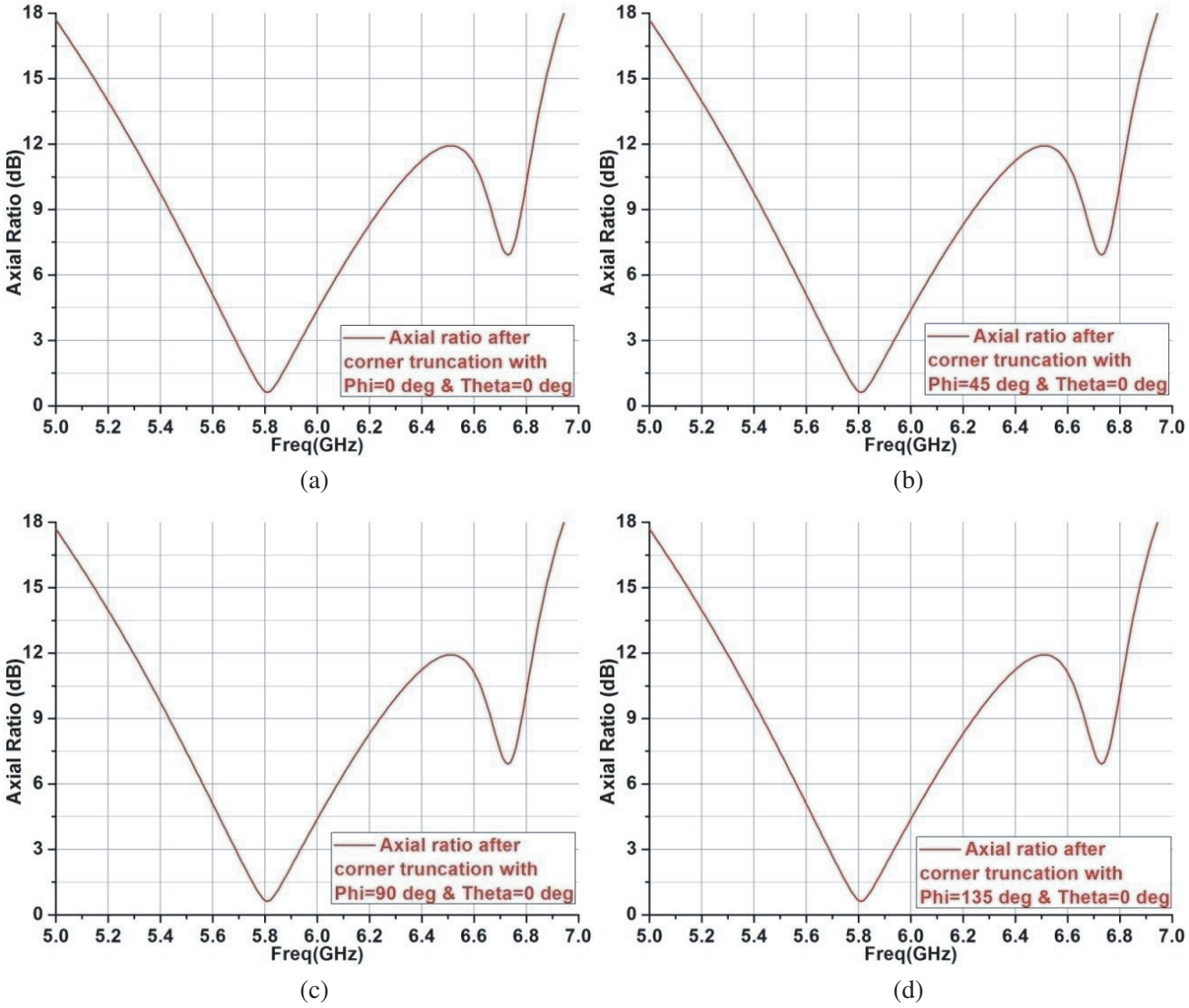

Figure 6. Simulated axial ratio with (a) Phi = 0 and Theta = 0 deg, (b) Phi = 45 and Theta = 0 deg, (c) Phi = 90 and Theta = 0 deg, and (d) Phi = 135 and Theta = 0 deg.

4. RESULTS

The simulated and measured results for different parameters of the designed antenna have been summarized in Table 1.

Graphs of different parameters with measured results are shown in Figs. 7, 8, 9, 10, 11, and 12.

From the above graphs shown in Figs. 7, 8, 9, 10, 11, and 12, it can be observed that the measured and simulated results match closely with a little shift in the measured results due to erroneous soldering of the connector with the ground and the patch of the antenna, impure substrate material, and inadequate measuring environment which is not considered during the simulation.

The radiation efficiency of an antenna is defined as the ratio of the power radiated by an antenna to the power fed to the antenna. From Fig. 10, a satisfactory radiation efficiency of more than 80% can be observed in the (5.69–5.93 GHz) resonant band. The total efficiency is the same as the radiation efficiency of the antenna if there is no loss due to impedance mismatch. The input impedance graph in Fig. 8 shows good impedance matching of the antenna in the desired resonant band. Therefore, total

Table 1.

Parameters	Simulated	Measured
Resonant band ($S_{11} \leq -10$ dB)	(5.38–6.90 GHz)	(5.40–6.89 GHz)
Impedance bandwidth ($S_{11} \leq -10$ dB)	1.52 GHz, 24.75%	1.49 GHz, 24.25%
Resonant band (Axial ratio ≤ 3 dB)	(5.69–5.93 GHz)	(5.71–5.95 GHz)
Circularly polarized bandwidth (AR ≤ 3 dB)	240 MHz, 4.13%	240 MHz, 4.11%
Peak Gain (dB)	4 dB at 5.81 GHz	3.9 dB at 5.81 GHz
Application	1. (5.725– 5.850 GHz) WLAN 2. (5.85–5.925 GHz) Dedicated short-range communication	

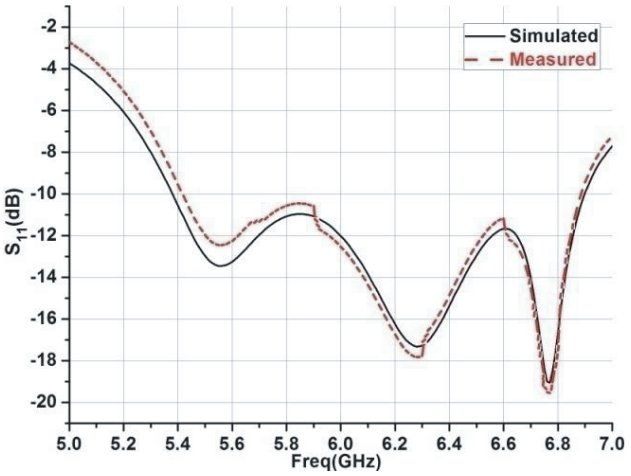

Figure 7. Measured and simulated S_{11}.

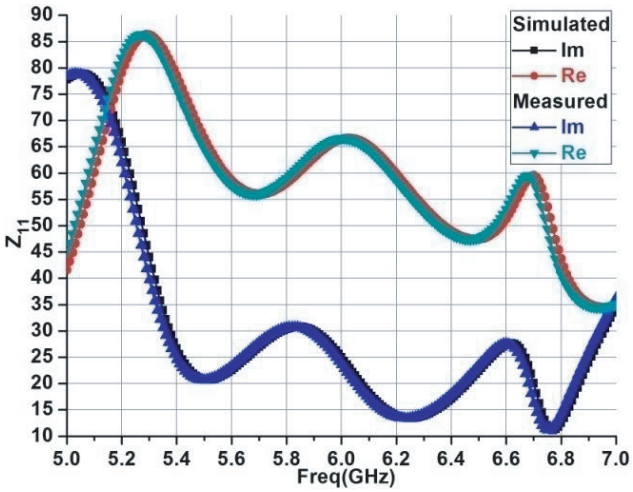

Figure 8. Measured and simulated input impedance.

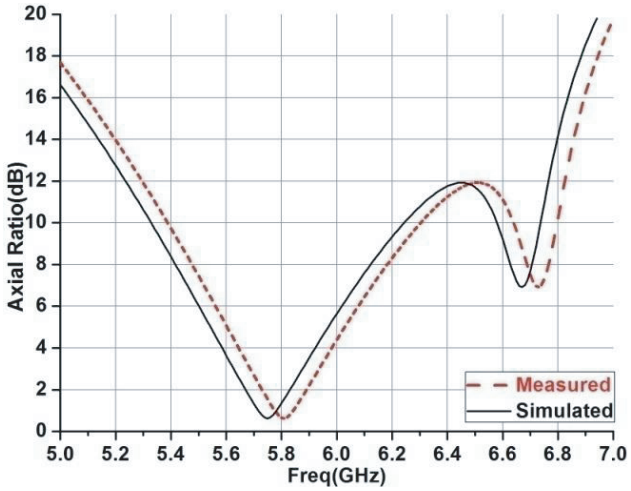

Figure 9. Measured and simulated axial ratio.

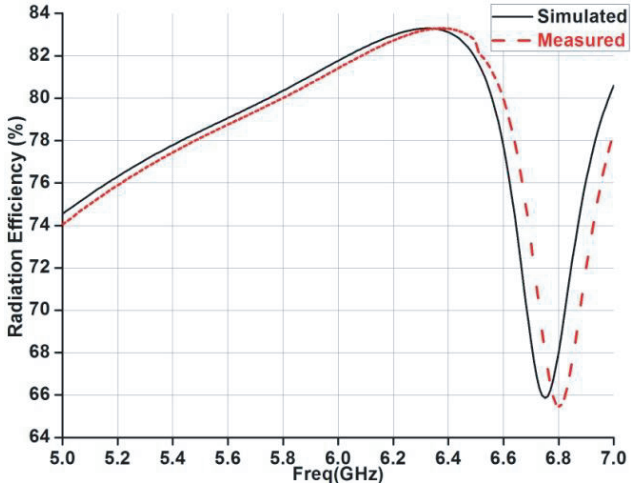

Figure 10. Measured and simulated radiation efficiency.

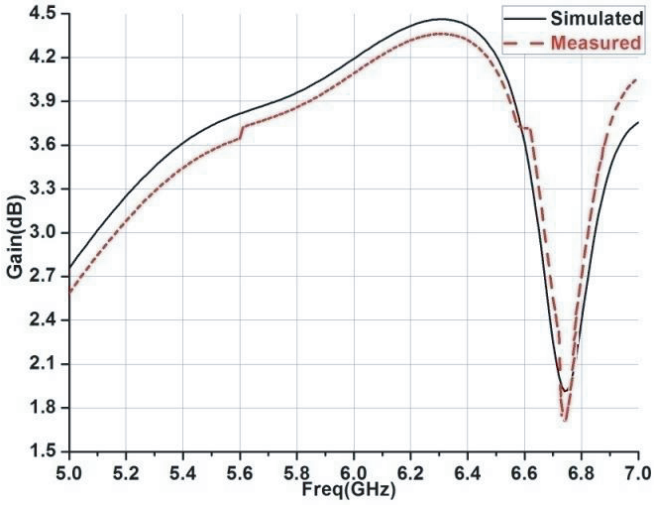

Figure 11. Measured and simulated gain.

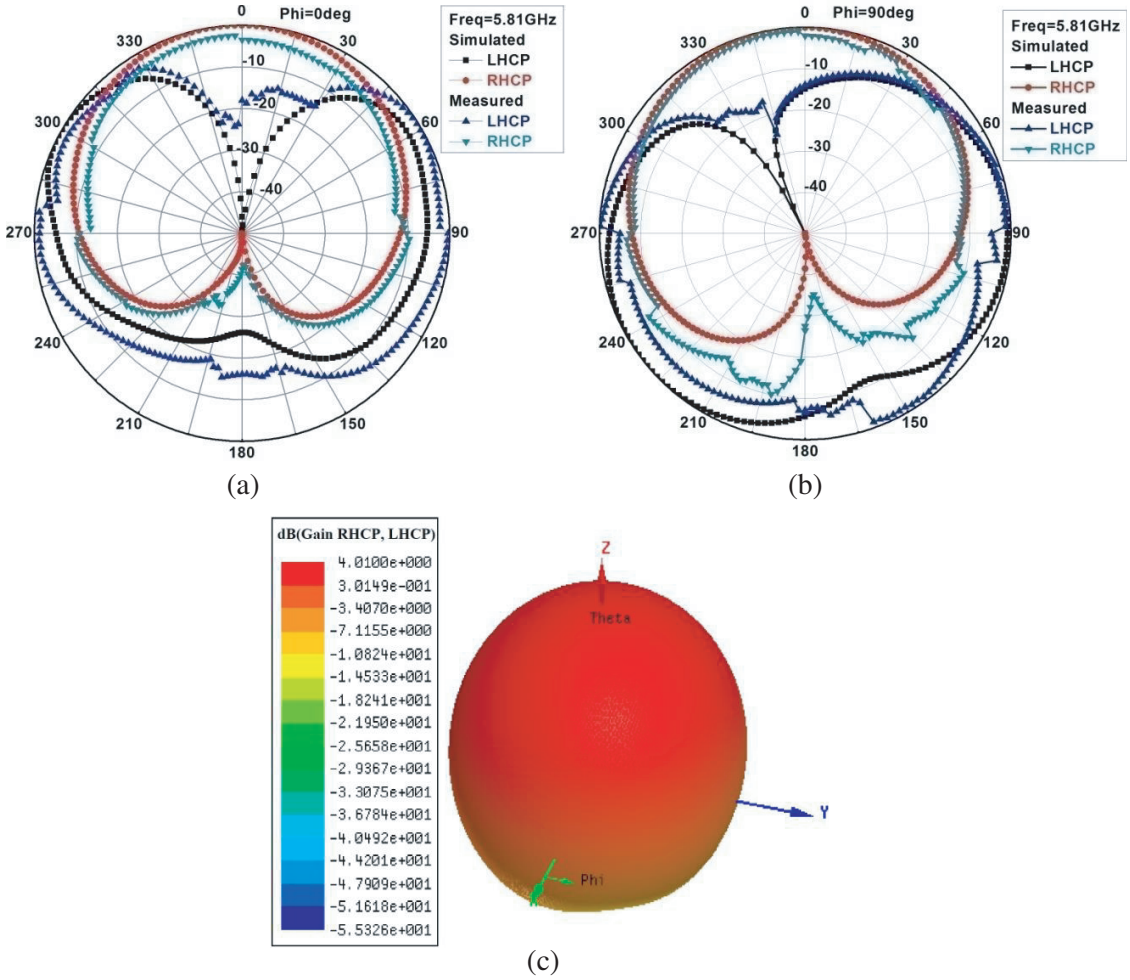

Figure 12. (a) Normalized radiation pattern in X-Z plane and (b) Y-Z plane at 5.81 GHz frequency. (c) Simulated 3D radiation pattern at 5.81 GHz frequency.

efficiency and radiation efficiency are almost the same for the proposed antenna.

The radiation pattern of a circularly polarized wave (RHCP and LHCP) is displayed in a two-dimensional (E & H) plane containing the electric field vector and magnetic field vector.

Figure 12 shows the simulated and measured radiation patterns with RHCP and LHCP at 5.81 GHz frequency with Phi = 0° and 90° and theta (O) between 0° and 360°. A circularly polarized antenna has either LHCP or RHCP gain greater than the other. The purity of the circular polarization is better with a higher difference between these two gains. From Fig. 12, it can be observed that the designed antenna is RHCP because the RHCP gain is higher than the LHCP gain. It can also be observed that there is a satisfactory difference in the gain between RHCP and LHCP.

Performance comparison of the proposed antenna with the previously available same type of antenna in literature is summarized in Table 2, which shows the merit of the proposed antenna.

Table 2. A comparison of the designed antenna performance with existing cases in the literature shows the merit of the proposed antenna.

Ref. No.	**Antenna size ($\lambda_0 \times \lambda_0 \times \lambda_0$)**	**Impedance Bandwidth ($S_{11} \leq -10$ dB)**	**Axial Ratio Bandwidth (AR $\leq$ 3 dB)**	**Gain**	**Application**
[30]	$(0.46 \times 0.46 \times 0.001)$ at 0.916 GHz	248 MHz 25%	27 MHz 3%	6 dBi	RFID
[31]	$(1.4 \times 1.4 \times 0.13)$ at 3.79 GHz	1.64 GHz 50.46%	—-	6.5 dBi	—-
[32]	$(0.93 \times 0.87 \times 0.013)$ at 2.45 GHz	22 MHz 2.5% 109 MHz 4.4%	—-	5, 8.8 dBi	RFID
[33]	$(0.48 \times 0.45 \times 0.03)$ at 2.6 GHz	550 MHz 23.25%	120 MHz 5.1% 40 MHz 1.54%.	4.54 dBic, 1.05 dBic	SDARS, LTE 2300
[34]	$(0.25 \times 0.25 \times 0.094)$ at 0.95 GHz	531 MHz 50.11%	49 MHz 5.23%	9 dBi	Mobile comm. system
[35]	$(7 \times 7 \times 0.12)$ at 23.525 GHz	—-	—-	—-	Satellite Comm.
[36]	$(2.05 \times 2.05 \times 2.05 \times 0.15)$ at 2.15 GHz	905 MHz 42.2%	—-	10.8 dBi	RF energy harvesting
This work	$(0.58 \times 0.58 \times 0.06)$ at 5.81 GHz	1.52 GHz 24.75%	240 MHz 4.13%	4 dB	WLAN DSRC

where, λ_0 is the free-space wavelength.

5. CONCLUSION

A low-profile microstrip patch antenna with broad circularly polarized resonant bandwidth has been proposed in this research work. The designed antenna in the proposed work covers a couple of application bands with satisfactory radiation pattern, gain, and radiation efficiency. A detailed introduction with an adequate literature review has been presented prior to the design process of the antenna. Next to the introduction, a complete design process has been described including a theoretical calculation using mathematical equations with proper reason and justification at every step of the process. After providing a detailed design process, the different parameters of the antenna have been given in a tabular form with both measured and simulated results. The merit of this antenna design is that almost all the modification has been done in parasitic elements with a little cut in one of the corners of the driver patch.

Therefore, no any major complex technique is used in the design which adds unnecessary complexity. Using this technique, more and more simple and low-profile antennas can be designed with differently shaped driver patches using modification in the parasitic elements. Hence, the proposed antenna is very much suitable as per the requirement of the advanced communication technology for low profile, low cost, circularly polarized bandwidth, use for more than one application band, and also fulfills low-cost commercial demand.

ACKNOWLEDGMENT

Heartly, thankful to Professor. (Dr.) Bhaskar Gupta and Joydeep Paul research scholar of Jadavpur University for using HFSS ver.13 software in their Lab. as well as the measurement of different parameters of fabricated antenna.

REFERENCES

1. Ojaroudi, Y., N. Ojaroudi, and N. Ghadimi, "Circularly polarized microstrip slot antenna with a pair of spur-shaped slits for WLAN applications," *Microwave Opt. Technol. Lett.*, 756–759, 2015.
2. Valizade, A., M. Ojaroudi, and N. O. Parchin, "CPW-fed small slot antenna with reconfigurable circular polarization and impedance bandwidth characteristics for DCS/WiMAX application," *Progress In Electromagnetics Research C*, Vol. 56, 65–72, 2015.
3. Ding, K., C. Gao, D. Qu, and Q. Yin, "Compact broadband circularly polarized antenna with parasitic patches," *IEEE Transactions on Antennas and Propagation*, Vol. 65, 4854–4857, 2017.
4. Sung, Y., "Circularly polarized patch antenna with two different C-shaped ring structures," *Microw. Opt. Techno. Lett.*, Vol. 61, 2773–2780, 2019.
5. Li, K., F. W. Wang, Y. H. Ren, and Y. M. Cai, "Dual band circularly polarized antenna with harmonic suppression performance," *Int. J. RF Microw. Comput. Aided Eng.*, Vol. 29, e21798, 2019.
6. Parchin, N. O., H. J. Basherlou, and R. A. Abd-Alhameed, "Dual circularly polarized crescent shaped slot antenna for 5G front-end systems," *Progress In Electromagnetics Research Letters*, Vol. 91, 41–48, 2020.
7. AI-Yasir, Y. I. A., O. P. Naser, A. Alabdullah, et al., "New pattern reconfigurable circular disk antenna using two PIN diodes for WiMax/WiFi (IEEE 802.11a) applications," *16th International Conference on Synthesis, Modeling, Analysis and Simulation Methods and Applications to Circuit Design (SMACD)*, 53–56, 2019.
8. Ullah, A., O. P. Naser, M. Alibakhshikenari, et al., "A circularly-polarized patch antenna design for 3.6 GHz applications in 5G systems," *International Telecommunications Conference (ITC-Egypt)*, 2023.
9. Chen, C.-H. and E. K. N. Yung, "Dual-band circularly-polarized CPW-fed slot antenna with a small frequency ratio and wide bandwidths," *IEEE Transactions on Antennas and Propagation*, Vol. 59, 1379–1384, 2011.
10. Chen, C.-H. and E. K. N. Yung, "Dual-band dual-sense circularly-polarized CPW-fed slot antenna with two spiral slots loaded," *IEEE Antennas and Wireless Propagation*, Vol. 57, 1829–1833, 2009.
11. Zhou, C., G. Wang, Y. Wang, B. Zong, and J. Ma, "CPW-fed dual-band linearly and circularly polarized antenna employing novel composite right/left-handed transmission-line," *IEEE Antennas and Wireless Propagation Lett.*, Vol. 12, 1073–1076, 2013.
12. Ryu, Y.-H., J.-H. Park, J.-H. Lee, and H.-S. Tae, "Multiband antenna using +1, −1, and 0 resonant mode of DGS dual composite right/left handed transmission line," *Microw. Opt. Technol. Lett.*, Vol. 51, 2485–2488, 2009.
13. Lu, J. H., C. L. Tang, and K. L. Wong, "Circular polarization design of a single-feed equilateral-triangular microstrip antenna," *Electronics Letters*, Vol. 34, 319–321, 1998.
14. Tang, C. L., J. H. Lu, and K. L. Wong, "Circularly polarized equilateral-triangular microstrip antenna with truncated tip," *Electronics Letters*, Vol. 34, 1277–1278, 1998.

15. Kuo, J. S. and G. B. Hsieh, "Gain enhancement of a circularly polarized equilateral-triangular microstrip antenna with a slotted ground plane," *IEEE Transactions on Antennas and Propagation*, Vol. 51, 1652–1656, 2003.
16. Nasimuddin, Z. N. Chen, and X. Qing, "A compact circularly polarized cross-shaped slotted microstrip antenna," *IEEE Antennas and Wireless Propagation*, Vol. 60, 1584–1588, 2012.
17. Yuandan, D., H. Toyao, and T. Itoh, "Compact circularly-polarized patch antenna loaded with metamaterial structures," *IEEE Antennas and Wireless Propagation*, Vol. 59, 4329–4333, 2011.
18. Lu, J. H. and K. L. Wong, "Single-feed circularly polarized equilateral-triangular microstrip antenna with a tuning stub," *IEEE Transactions on Antennas and Propagation*, Vol. 48, 1869–1872, 2000.
19. Hassani, H. R. and D. M. Syahkal, "Analysis of triangular patch antennas including radome effects," *IEE Proceedings — H*, Vol. 139, 251–256, 1992.
20. Wong, K. L. and W. H. Hsu, "Broadband triangular microstrip antenna with U-shaped slot," *Electronics Letters*, Vol. 33, 2085–2087, 1997.
21. Biswas, M. and M. Dam, "Characteristics of equilateral triangular patch antenna on Suspended and Composite Substrates," *Electromagnetics*, Vol. 33, 99–115, 2013.
22. Kumprasert, N. and W. Kiranon, "Simple and accurate formula for the resonant frequency of the equilateral triangular microstrip patch antenna," *IEEE Transactions on Antennas and Propagation*, Vol. 42, 1178–1179, 1994.
23. Wang, J., Q. Liu, and L. Zhu, "Bandwidth enhancement of a differential-fed equilateral triangular patch antenna via loading of shorting posts," *IEEE Transactions on Antennas and Propagation*, Vol. 65, 36–43, 2017.
24. Kamalaveni, G. and M. G. Madhan, "A compact parasitic ring antenna for ISM band applications," *Frequenz*, Vol. 70, 513–519, 2016.
25. Lu, H. X., F. Liu, M. Su, and Y. A. Liu, "Design and analysis of wideband U-slot patch antenna with U-shaped parasitic elements," *Int. J. of RF and Microw. Comp.-Aided Eng.*, Vol. 28, e21202, 2017.
26. Kumar, S., R. K. Viswakarma, R. Kumar, J. Anguera, and A. Andujara, "Slotted circularly polarized microstrip antenna for RFID application," *Radioengineering*, Vol. 26, 1025–1032, 2017.
27. Sung, Y., "Axial ratio-tuned circularly polarized square patch antenna with long stubs," *Int. J. of Antennas and Propagation*, Article ID 7068560, 1–7, 2018.
28. Saraswat, K., T. Kumar, and A. R. Harish, "A corrugated G-shaped grounded ring slot antenna for wideband circular polarization," *Int. J. of Microw. and Wireless Technol.*, Vol. 12, 1–6, 2019.
29. Al-Yasir, Y. I. A., N. O. Parchin, I. Elfergani, et al., "A new polarization-reconfigurable antenna for 5G wireless communications," *Broadband Communications, Networks, and Systems*, 431–437, Cham, Faro, Portugal, 2019.
30. Yeh, C. H., Y. W. Hsu, and C. Y. D. Sim, "Equilateral triangular patch antenna for UHF RFID applications," *Int. J. of RF and Microw. Comp.-Aided Eng.*, Vol. 24, 2014.
31. Wang, J., Q. Liu, L. Zhu, "Bandwidth enhancement of a differential-fed equilateral triangular patch antenna via loading of shorting posts," *IEEE Transactions on Antennas and Propagation*, Vol. 65, 36–43, 2017.
32. Tiang, J. J., M. T. Islam, N. Misran, and J. S. Mandeep, "A rounded corner triangular patch antenna for dual frequency application," *Microwave Opt. Technol. Lett.*, Vol. 56, 2014.
33. Shaw, M., N. Mandal, and M. Gangopadhyay, "A compact circularly polarized isosceles triangular microstrip patch antenna with parasitic elements for multiband application," *Microw. Opt. Technol. Lett.*, 1–8, 2020.
34. Deshmukh, A. A., A. Doshi, P. D. I. Kamble, and K. P. Ray, "Modified triangular shape microstrip antenna for circular polarization," *Procedia Computer Science*, Vol. 115, 108–114, 2017.
35. Siddiqui, M. G., A. K. Saroj, Devesh, and J. Ansari, "Multi-band fractaled triangular microstrip antenna for wireless applications," *Progress In Electromagnetics Research M*, Vol. 65, 51–60, 2018.
36. Chopra, R. and G. Kumar, "High gain broadband stacked triangular microstrip antennas," *Microw. Opt. Technol. Lett.*, 1–8, 2020.